Monatshefte für Chemie 132, 1295–1326 (2001)

Monatshefte für Chemie
Chemical Monthly

Invited Review

Recent Advances in the Description of the Structure of Water, the Hydrophobic Effect, and the Like-Dissolves-Like Rule

Roland Schmid*

Institute of Inorganic Chemistry, Technical University of Vienna, A-1060 Vienna, Austria

Summary. Following a critical survey of the vast recent literature, the state of the art may be summarized as follows:

(A) Water structure. The key is appreciating the next-nearest neighbour aspect. Thus, liquid water may be conceived as a fluctuating mixture of broadly two groups of structure elements: (*i*) an open ice-I_h-type outer neighbour O···O bonding at about 4.5 Å and (*ii*) a dense ice-II-type outer neighbour O···O bonding at about 3.4 Å. On the other hand, the nearest neighbour O···O distance of about 2.8 Å and the number of these neighbors (4) is very similar in the solid and liquid state. The characterization of the two states may be directed either by the geometry of the H-bonds (more linear H-bonds in (*i*) and more bent H-bonds in (*ii*) or by the bonding forces operating (H-bonding favours the ordered open state (*i*), oxygen–oxygen interactions favour the random dense state (*ii*). Basically, the nature of liquid water can be understood in terms of a competition between H-bond (*Coulomb*) and dispersion (*van der Waals*) forces. Since the bonding characteristics in crystalline phases carry over to the liquid state, any molecular dynamics (MD) model of the liquid would have first of all to reproduce well the ice polymorph structures under appropriate thermodynamic conditions.

(B) Hydrophobic effect. The two classic approaches, *i.e.* the clathrate cage model and the cavity-based model, appear to be just different perspectives on the same physics. The particular features of water are (*i*) the small molecular size or, more specifically, the small size of the space between water molecules and the low expansibility, and (*ii*) the structure of the water molecule with the same number of donor and acceptor sites arranged tetrahedrally. Due to (*i*), cavity formation is particularly demanding, and this is the main contributor to the hydrophobic effect. This is mitigated by the capability of water, due to (*ii*), to form a cage around a nonpolar solute without sacrificing much of the H-bonding; rather, H-bonding networks are stabilized by the presence of guest molecules. In view of the tangential orientation of the first-sphere waters, such a cage can be compared with an elasticated net effecting strong solute–solvent dispersive interactions, rendering the solubility of nonpolar gases exothermic at room temperature. Furthermore, cavity formation largely determines the excess entropy, whereas dispersive forces determine the excess enthalpy. This gives rise to compensation behaviour when the solute size varies. Whereas an increase in solute size enhances the cavity formation energy, polarizability is also increased, and this leads to stronger solute–water interaction. Unfortunately,

* E-mail: rschmid@mail.zserv.tuwien.ac.at

present models of cavity formation predict positional entropies that are far in excess of the experimental entropies so that orientational contributions due to cage formation are hard to accommodate.

(C) Like-dissolves-like rule. The number of exceptions is dramatically reduced if the term polarity is given a broader meaning. Instead of identifying it solely with dipolarity, it should also include higher multipolar properties, in particular quadrupolarity. Quadrupolar solvent effects on solvation and reactivity are receiving increasing attention, particularly in low dielectric solvents.

Keywords. Water structure; Hydrophobic effect; Cavity formation; Solvent reorganization energy; Compensation effect; Quadrupolar solvents.

Introduction

Hydrophobicity is, without doubt, one of the most widely discussed features of contemporary solution chemistry and biochemistry. It is invoked in treating phenomena as different as the cleaning action of soaps and detergents, the influence of surfactants on surface tension, the immiscibility of nonpolar substances with water [1], the formation of biological membranes and micelles [2, 3], the folding of biological macromolecules in water [4], clathrate hydrate formation [5], and the binding of a drug to its receptor [6]. Besides, hydrophobic interactions are considerably involved in self-assembly, leading to the aggregation of nonpolar solutes or, equivalently, to the tendency of nonpolar oligomers to adopt chain conformations in water relative to a nonpolar solvent [7].

Due to these wide span of applications, the hydrophobic effect has often been separated into two categories: hydrophobic hydration describing structural and dynamic changes of water around a nonpolar solute, and hydrophobic interaction referring to the tendency of nonpolar solutes to aggregate in aqueous solution. In these terms, the latter category can be viewed as the reverse of the former.

Historically, the concept of hydrophobicity arose in the context of the low solubility of nonpolar compounds in water. Thus, unlike simple organic solvents, the insertion of a nonpolar solute into water at room temperature is (1) strongly unfavourable though slightly favoured by enthalpy, but (2) strongly opposed by a large, negative change in entropy, and (3) accompanied by a large positive heat capacity. An example is given in Table 1 showing the thermodynamic properties of methane dissolved in water and in carbon tetrachloride. In general, the solubility of nonpolar gases in water is 1 to 3 orders of magnitude smaller than in common hydrocarbon liquids [8]. Formerly unaware of the importance of dispersion (*van der Waals* (*vdW*), nonbonded) interactions, these thermodynamic characteristics were interpreted in terms of the formation of an ordered structure of water (an

Table 1. Solution thermodynamics of methane in water and carbon tetrachloride at 25°C; data are taken from *Lazaridis T*, *Paulaitis ME* (1992) J. Phys. Chem. **96**: 3847 and Ref. [67]

	Water	CCl_4
ΔG/kJ · mol^{-1}	+8.4	+0.9
ΔH/kJ · mol^{-1}	−10.9	−1.2
ΔS/J · mol^{-1} · K^{-1}	−64.6	−7.1
$298\Delta S$/kJ · mol^{-1}	−19.2	−2.1
ΔC_p/J · mol^{-1} · K^{-1}	217.5	(0 to 42)

Table 2. Change in the solution thermodynamics of methane in water with temperature; data are taken from Ref. [142b]

	25°C	65°C	160°C
ΔG/kJ · mol^{-1}	8.4	10.5	17.4
ΔH/kJ · mol^{-1}	−10.9	−2.3	+11.3
ΔS/J · mol^{-1} · K^{-1}	−64.6	−37.7	−14.1
$T\Delta S$/kJ · mol^{-1}	−19.2	−12.8	−6.1

iceberg) around the nonpolar solute, which, though exothermic, is entropically unfavourable. It should be emphasized, however, that (due to the large positive heat capacity change involved) both heat and entropy of solvation are strongly temperature dependent. As is shown in Table 2, the large positive free energy of mixing of hydrocarbons with water is dominated by entropy only at ambient temperatures, whereas it is dominated by enthalpy at higher temperatures where the disaffinity is enlarged. Paradoxically, where hydrophobicity is strongest, entropy plays a minor role. Consequently, models that focus on water at around room temperature miss much of the thermodynamics of the oil/water solvation process. In addition, since the hydration of any solute – polar, nonpolar, or ionic – is accompanied by a decrease in entropy [9], the negative entropy of hydration is arguably not the main characteristic feature of hydrophobicity. The qualitative similarity in the hydration entropy behaviour of polar and nonpolar groups contrasts sharply with the opposite sign of the heat capacity change in polar and nonpolar group hydration. Nonpolar solutes have a large positive heat capacity of hydration, whereas polar groups have a smaller negative one. Thus, the large heat capacity increase might be what truly distinguishes the hydrophobic effect from other solvation phenomena [10].

Indeed, thermodynamic observables reflect bulk or averaged quantities. Thus, with the advent of computer simulation techniques (molecular dynamics (MD), Monte Carlo (MC)) every endeavour has been made to decipher features that are not directly measurable. After three decades of such studies it appears that simulation of chemical systems is a powerful way of gaining information on the atomic scale. However, the prolific literature devoted to simulations of water and aqueous solutions is increasingly hard to survey. In addition, several theoretical approaches to solvation exist, and the correspondence between the various terms appearing in different theories is not clear. Furthermore, establishing a connection between theoretical terms and the many intuitive ideas about solvation has proved to be difficult. Consequently, different qualitative conclusions have frequently been drawn as to the physical origin of hydrophobicity.

Another source of confusion is that because solvation is complex, insights are commonly obtained by studies of simpler reference fluids. The conclusions drawn from these studies are then extrapolated to real fluids. Since there is no unique way of doing this, the results may differ depending on the scheme of extrapolation adopted [11]. For all these reasons, there are currently many contradictory papers on the subject. Thus, in a quite recent communication [12] it is claimed that water should not be blamed for the hydrophobic effect. Instead, the formation of molecular aggregates is not limited to aqueous solutions, but it is a universal

phenomenon associated with appreciably non-ideal solutions. The history of the study of the hydrophobic effect is in fact a vivid example of a tenet given by *Bertrand Russell* saying: ''Unless we can know something, without knowing everything, it is obvious that we never know something.''

It is therefore appropriate to review the subject with emphasis placed on publications that have appeared since the review by *Blokzijl* and *Engberts* in 1993 [13]. The review of the present author may also be noted [14]. It should be stressed here that the vast literature on the topic is virtually impossible to survey comprehensively. In what follows only a few papers (and references therein) that have paved the way to the present state of the art will be cited. It is not intended just to give an overview of existing ideas, but to sort out facts and fiction, both experimental and theoretical. It should be mentioned that this study is restricted to the phenomenon of hydrophobic hydration, thus omitting hydrophobic interaction.

Structure of Liquid Water

Crucial for all aspects of aqueous chemistry is an understanding of the structure of water itself. In a liquid, molecules are in constant motion and do not have fixed positions and orientations. Therefore, any structure of the liquid must be described in terms of probabilities and averages. The numerous models for water structure proposed so far fall into two main classes: continuum and mixture models, differing basically in their perception of the hydrogen bonds. The former suggests almost completely H-bonded molecules in a continuous network where distortion of the H-bonds results in a smooth distribution of H-bond distances, angles, and energies. In this case, there should be a one-peak distribution of H-bond strengths and geometries. *Giguère*, therefore, termed this model 'uniformist' [15]. However, this scheme is incompatible with both the physical properties of water and its behaviour manifested in (properly disentangled) high-resolution *Raman*, near IR, and neutron scattering spectra. For the former, the (roughly ten) thermodynamic and kinetic anomalies, such as the density maximum at 4°C, and the compressibility minimum at 45°C, cannot be explained. From spectroscopic results, there is evidence of an equilibrium between broadly two different groups of water structural elements as follows.

Raman studies on water as a solvent go back at least to 1965 when *Wall* and *Hornig* obtained a single broad OD band displaying only slight asymmetry [16]. Lack of evidence for two or more distinct peaks caused them to favour an interpretation involving a continuum distribution of hydrogen bond properties. *Walrafen's* subsequent work at higher resolution displayed an asymmetry more clearly [17]. In addition, he obtained a frequency of temperature independent intensity, that is, an isosbestic crossing of isotherms. Such a behaviour is indicative of a system composed of two distinct classes of scatters as has subsequently been supported by *d'Arrigo* and coworkers [18], *Giguère* [19], *Walrafen* and coworkers [20], and *Hare* and *Sørenson* [21].

Further evidence of a two-state system stems from mid-infrared spectroscopy, *i.e.* absorption spectroscopy of fundamental (0→1) vibrational transitions, and this may be considered one of the most powerful techniques in the study of H-bonds. However, the strong absorbance of the fundamental OH stretching gives rise to

intense broad bands, prohibiting the derivation of reliable quantitative structural information from this region with standard infrared techniques. Fortunately, new techniques such as attenuated total reflection (ATR) allow to avoid saturation effects. Such ATR spectra recorded by *Maréchal* as a function of temperature can be decomposed into two spectra, a low temperature one and a high temperature one [22]. The same result has been derived from ATR infrared measurements resolved by evolutionary curve resolution [23].

A particularly intriguing case is the advancement of the interpretation of X-ray and neutron diffraction experiments for obtaining atom-atom radial distribution functions (RDFs) $g(r)$ in water. Such measurements can reveal the local coordination structures of molecules in liquids. According to a classical integration procedure, the O–O distribution has a well-defined peak at 2.975 Å consisting of *ca*. 4.5 oxygen atoms out to a distance of 3.3 Å from an oxygen atom at the origin [24]. These numbers and distances suggest that the near neighbor coordination of water molecules is well defined and roughly tetrahedral at any instant in time but that a substantial number of molecules (in the order of 10%) are to be found in other configurations. The location of the first minimum in the O–O RDF around 3.3 Å is usually used to define the hydrogen bond. Thus, two water molecules are commonly considered to be H-bonded if their O–O distance is less than or equal to this distance. There was a long-standing debate as to whether the local pair density in water at interparticle separations of about 3.5 Å originates from large fluctuations in the separation of first H-bonded neighbours, from indirect second-neighbor correlations in small four- and five-membered rings, or from the distinct so-called interstitial fraction of water molecules. In fact, any RDF is the one-dimensional representation of a three-dimensional structure (and as such spatially averaged) and therefore carries a limited amount of structural information. Consequently, more recent simulation [25, 26] and experimental studies [27] employ orientation resolved spatial distribution functions (SDFs) to clarify the structural behaviour. In another paper [28], molecular orientations have been defined using *Eulerian* angles.

Notwithstanding, a look at the X-ray RDFs for liquid water suggests that the first peak cannot fit well a single *Gaussian* curve. The asymmetry towards longer distances increases with temperature, pointing at another overlapped $O \cdots O$ peak, and, therefore, a more complex first coordination sphere of the water molecule [29]. That feature had already been considered in 1962 by *Némethy* and *Scheraga* [30] on the basis of the X-ray diffraction patterns of amorphous ice, where the two peaks are well resolved. A final corroboration of this idea was provided by *Bosio*, *Chen*, and *Teixeira* [31] who introduced, for the study of liquid heavy water, a new approach. Making use of the water's maximum in the temperature-density curve (at 11.2°C), measurements of the X-ray structure factor can be performed at pairs of temperatures around the maximum at which the density is a constant. By subtracting the respective RDFs they obtained isochoric temperature differentials (ITD). In this way the temperature dependence of the structural parameters can be obtained much more precisely, since many density dependent corrections are circumvented. It was then shown [32] that these ITDs display the remarkable property that only the heights of the maxima and minima, but not their positions, depend on temperature. This is interpreted to mean that the water molecules exist

in two distinct configurations characterized by either four or five neighbours. A summary of the various types of isosbestic points found for the structural changes of water with variable temperature and pressure, which is strong evidence for a two-state mixture model, has been given very recently [33].

In structural terms, the results from the ITD measurements reveal that it is not adequate to consider the coordination number of water as 4.5. Rather, it is essential to differentiate between first-neighbour and second-neighbour coordination. There are a nearest-neighbour O···O distance of about 2.8 Å and at least two outer-neighbour O···O distances, one of about 3.3 Å, whose intensity grows with increasing temperature, and one near 4.5 Å, which decreases with temperature. The interpretation of these distances in terms of chemical bonding is straightforward through their close relationship with the radial distribution functions of the various forms of ice in combination with the corresponding crystal structures. In fact, as pointed out by *Kamb* and referred to by *Robinson* and coworkers [34], the RDFs of the liquid can be created by a superposition of ice-I_h, -II, and -III RDFs (the subscript h means hexagonal). In other words, the bonding characteristics in crystalline phases carry over to the liquid state, a reasonable feature indeed. Most intriguing is the 3.3 Å distance which does not occur at all in ice-I structures but is very close to prominent features in ice-II, -III, -V, and -VI.

Ice-II, formed from ice I by raising the pressure to about 3 kbar at temperatures around −60°C, is taken as a case study. According to *Kamb* [35, 36], the structure of ice-II can be derived from ice-I as follows: detach the hexagonal columns of ice-I from one another, move them relatively up and down parallel to the long hexagonal axis so as to give a rhombohedral stacking sequence for equivalent six-rings, rotate them by *ca.* 30° around this axis, and finally re-link them together in a more tightly fitting way than in ice-I. As a result, each oxygen is bonded to four nearest neighbours at 2.77–2.82 Å and has, in addition, a next-nearest neighbour at 3.24–3.60 Å, which is not H-bonded to the central water molecule. This is shown in Fig. 1. In ice-I_h, in comparison, there is the same nearest neighbour O···O distance of 2.75 Å, whereas the next-nearest neighbour is 4.5 Å away from the center. Another difference between ice-I_h and ice-II is the O···O···O angle

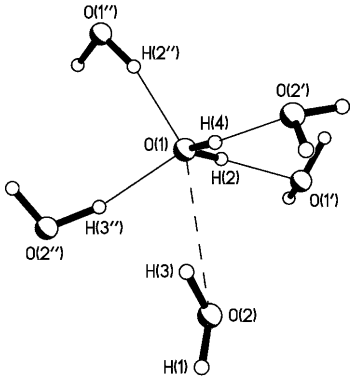

Fig. 1. Structure element of ice-II showing the next neighbours of a water molecule. Each of the four nearest oxygen atoms, at distances of 2.77–2.84 Å, is linked by a hydrogen bond. The fifth oxygen atom is non-H-bonded with an O(1)–O(2) distance of 3.24 Å. Data are taken from Ref. [36]

(*i.e.* O···H–O–H···O), which is 109.5° in the former but 93.8° (average) in the latter. Thus, H-bonds are linear in ice-I, but appreciably bent in ice-II. In liquid water, both features are simultaneously present.

It should be stressed, however, that water should not be conceived as some sort of mixture of ices, but rather is a rapidly (on picosecond timescales) fluctuating mixture of the intermolecular bonding types found in the polymorphs of ice. This two-state mixture model differs fundamentally from the traditional two-species mixture model, which considers liquid water as a mixture, or solution, of at least two molecular species, such as tetramers and octamers [37], distinguishable by the number of H-bonds. This latter model implies the concept of broken H-bonds (whose nature has never been defined) and estimates of their concentration in water, based on various criteria, diverge over an excessively wide range [38]. In fact, the presentation of diffraction data by orientational correlation functions shows that there are a range of local orientations compatible with the neutron data. This argues against the notion of water forming short lived, ice-like clusters at ambient temperature and pressure [27]. Furthermore, according to more recent *Raman* spectroscopic work [39], the concentration of free OH groups is only of the order of 1–2% by comparison with the spectra of the hydroxyl ion in aqueous solution. Therefore, some authors introduced the concept of the bifurcated H-bond, for which a hydrogen atom is bonded to three oxygen atoms [19]. This is another kind of molecular interaction, intermediate between the linear H-bond and the free OH group. It should be noted, however, that there is no suggestion of bifurcation of any of the H-bonds in ice-II.

Summing up, water may well be interpreted as a mixture of ice-I_h and ice-II type (representing all the other ice polymorphs) bonding, with average compositions depending on temperature and pressure. With increasing temperature or pressure, a transformation on the average occurs from the capacious, more rigid I_h-type outer-neighbour O···O bonding at 4.5 Å to the dense, more fragile II-type outer-neighbour O···O bonding near 3.4 Å. This implies that the bonding differences between the two states are not at the nearest-neighbour level but occur instead in the outlying non-hydrogen bonded next-nearest neighbour O···O structure. As in the polymorph structures, the transformation takes place by a bending of the inner-neighbour H-bonds without appreciably changing neither the O···O nearest neighbour distances of about 2.8 Å, nor the number of these neighbours (four).

The characterization of the two states may be directed either by the nature of the H-bonds or by the bonding forces operating. For the former, the dense and the capacious states involve linear and bent H-bonds, respectively. The latter definition is more fundamental, referring to a competition between O–O *vdW* interactions that favour random dense states and H-bonding that favours ordered open states. In this way the peculiarities of water are adequately captured: they are not simply due to H-bonding interactions, but rather to the admixing of trivial nondirectional *vdW* forces holding otherwise together the regular or unstructured liquids. It is intriguing to speculate that *vdW* interactions are necessary to offset energy losses caused by H-bonds bending to form the much more compact O···O···O angles [40]. Note that the low density of ice is due to the fact that H-bonding is stronger than *vdW* interactions. Optimal H-bonding is incommensurable with the tighter packing that would be favoured by *vdW* interactions. Ice melts when the thermal

energy is sufficient to disrupt and disorder the hydrogen bonds, broadening the distribution of H-bond angles and lengths. Now among this broadened H-bond distribution, the *vdW* interactions favour those conformations of the system that have higher density. Hence, liquid water is denser than ice. In this framework all anomalies of water can be accommodated [40]. The density maximum, for instance, occurs due to the superposition of the open → dense transformation and normal thermal expansion when the temperature is raised.

These features are reflected by potential models used for the molecular dynamics simulation of liquid water of the form of Eq. (1) [28, 41], combining a *Lennard-Jones* (*LJ*) interaction between oxygen atoms with an electrostatic interaction modeled by interactions of point charges (q_i is the number of elemental charges in the i^{th} site). On the other hand, it has been shown that a solute-hydrogen potential function need not be included [42].

$$V = 4\varepsilon\left(\left(\frac{\sigma}{r_{\text{oo}}}\right)^{12} - \left(\frac{\sigma}{r_{\text{oo}}}\right)^{6}\right) + \frac{1}{4\pi\varepsilon_0}\sum_{i,j}\frac{q_i q_j e^2}{r_{ij}} \tag{1}$$

Hydrophobic Hydration

Ever increasing theoretical work within the last years has been devoted towards lifting the veil of secrecy about the molecular details of the hydrophobic effect, a subject of vigorous debate. Specifically, the scientific community would eagerly like to learn about the relative contributions of water-water and water-solute correlations to the thermodynamics of solution of nonpolar substances in water. Overall, there are two concepts: the older one clathrate cage model reaching back to the iceberg hypothesis of *Frank* and *Evans* [43], and the newer cavity based model.

The clathrate cage model assigns the responsibility of the low solubility of nonpolar solutes in water solely to the hydrogen bonding of water. In these terms, the structure of water is strengthened around a hydrophobic solute in order to avoid wasting hydrogen bonds. This causes a large unfavourable entropic effect, because the surrounding water molecules adopt only a few orientations (low entropy), with all water configurations fully H-bonded (low energy). Experimental evidence of structure strengthening is claimed to stem from NMR and FT-IR studies [44], NMR relaxation [45], dielectric relaxation [46], and HPLC [47].

In the cavity based model, the hard core of water molecules is more important to the hydrophobic effect than H-bonding of water. The process of solvation is dissected into two components: the formation of a cavity in the water to accommodate the solute and the interaction of the solute with the water molecules. The creation of a cavity reduces the volume of the translational motion of the solvent particles. This causes an unfavourable entropic effect. Thus, large perturbations in water structure are not required to explain hydrophobic behaviour. This conclusion arose from the surprising success of the scaled particle theory (SPT) which is a hard-sphere fluid theory, to account for the free energy of hydrophobic transfers. Since the theory only uses the molecular size, density, and pressure of water as input and does not explicitly include any special features of H-bonding of water, the structure of water is arguably not directly implicated in the hydration thermo-

dynamics; however, the effect of the H-bonds of water is implicitly taken into account through the size and density of water. The proponents of this hypothesis argue that the entropic and enthalpic contributions arising from the structuring of water molecules largely compensate each other. In fact, there are several papers propagating exact enthalpy-entropy compensation of solvent reorganization [48–51]. Likewise, recent simulations [52, 53] and neutron scattering data [54–56] suggest that solvent structuring might be of much lower extent than previously believed. Also, a recent MD study report [57] stated that the structure of water is preserved, rather than enhanced, around hydrophobic groups.

Since there is strong evidence for both models, the importance of water structure enhancement has been rather equivocal. The reason for this is at least twofold. Firstly, theoretical models have many adjustable parameters, so their physical bases are not always clear; additionally, MD simulations usually do not take into consideration the aforementioned next-nearest neighbour aspect of liquid water. This raises serious questions about the realism of the results. Any MD model of the liquid would have first of all to reproduce well the ice polymorph structures under appropriate thermodynamic conditions. Secondly, the free energy alone masks the underlying physics in the absence of a temperature dependence study because of the entropy-enthalpy compensation.

Notwithstanding these difficulties, it appears that the two approaches, the clathrate cage model and the cavity based model, are just different perspectives of the same physics with different diagnostics reporting consequences of the same shifted balance between H-bonds and *vdW* interactions. Actually, in a very recent paper, a unified physical picture of hydrophobicity based on both the hydrogen bonding of water and the hard-core effect has been put forward [58]. Thus, hydrophobicity features an interplay of several factors. In the following the state of the art of cavity formation, solute-water correlations, and entropy-enthalpy compensation will be delineated. First, the different reference states used in the literature and their conversions will be briefly outlined, since from that side the issue has been unnecessarily obscured.

Standard states

There are numerous ways of expressing the solubility of a gas in a liquid. Of these, the *Ostwald* solubility L, or gas-liquid partition coefficient, is an especially useful measure. It is defined as the ratio of the concentration of gas molecules B dissolved at equilibrium in the liquid solvent to their concentration in the gas phase. In other words, L is the ratio of the number densities

$$L = \frac{[\mathrm{B}_s]}{[\mathrm{B}_g]} = \frac{\rho_{\mathrm{B}}^l}{\rho_{\mathrm{B}}^g} = \frac{\textit{volume of absorbed gas}}{\textit{volume of solvent}} \tag{2}$$

where ρ_{B}^l and ρ_{B}^g are the number densities of the solute B in the liquid (l) and the gaseous (g) phases, respectively. The standard states implied in this case are

$$\mathrm{B}(\text{ideal gas}, C_{\mathrm{g}} = 1) \rightarrow \mathrm{B}(\text{ideal solution}, C_{\mathrm{s}} = 1) \tag{I}$$

and

$$-RT\ln L = \Delta G_{\mathrm{s}} \tag{3}$$

where ΔG, henceforth, is equivalent to ΔG^* in *Ben-Naim*'s notation [59]. It is perhaps ironic to find that the directly measured quantity has the physically reasonable standard state involved, but formerly many authors proceeded to convert the primary data into less informative quantities. A frequently used standard state refers to gas at 1 atm and to a solution of unit mole fraction [60],

$$\begin{array}{ccc} \mathrm{B(ideal\ gas, 1\ atm)} & \rightarrow & \mathrm{B(ideal\ solution}, x_\mathrm{B} = 1) \\ G_g = G_g^\circ + RT\ln(p/p_0) & & G_l = G_l^\circ + RT\ln x_\mathrm{B} \end{array} \qquad \text{(II)}$$

and

$$\begin{array}{cc} G_l - G_g = G_l^\circ - G_g^\circ + RT\ln(x_\mathrm{B} \cdot p_0/p) \\ \Delta G \qquad\quad \Delta G^\circ \end{array}$$

For $p = p_0$,

$$\Delta G = \Delta G^\circ + RT\ln x_\mathrm{B} \tag{4}$$

The additional approximation of Eq. (5) is now applied,

$$x_\mathrm{B} = \frac{n_\mathrm{B}}{n_\mathrm{B} + n_\mathrm{A}} \approx \frac{n_\mathrm{B}}{n_\mathrm{A}} \tag{5}$$

where n_A is the mole fraction of the solvent. Now taking the volume per mole of ideal gas RT/p for n_A, and the molar liquid volume V_l for n_A, one obtains $\Delta G = \Delta G^\circ + RT\ln(RT/pV_\mathrm{l})$, where p is the external pressure. Since, however, the latter term is included in ΔG°, it has to be subtracted in order to arrive at ΔG, *i.e.*

$$\Delta G = \Delta G^\circ + RT\ln(pV_\mathrm{l}/RT) \tag{6}$$

Thus, for water at 25°C,

$$\Delta G = \Delta G^\circ - 17.87\,\mathrm{kJ} \tag{7a}$$

$$\Delta S = \Delta S^\circ + 68.27\,\mathrm{J} \tag{7b}$$

Furthermore, since $\partial(RT\ln(pV/RT)/\partial T = R\ln(pV/RT) - R$, it follows that $\Delta H = \Delta H^\circ + RT$, *i.e.*

$$\Delta H = \Delta H^\circ + 2.48\,\mathrm{kJ} \tag{7c}$$

It should also be realized that the concept of the standard state (II) is not internally consistent since Eq. (5) implies a highly dilute solution, whereas the standard state refers to the neat solute [61].

Another outmoded standard state is [62]

$$\mathrm{B(ideal\ gas, 1\ atm)} \quad \rightarrow \quad \mathrm{B(ideal\ solution}, C_\mathrm{s} = 1) \qquad \text{(III)}$$

In converting reference state (III) into (I), the gas phase has to be compressed from 1 mol gas present in 24.46 dm^3 (at 298 K) to 1 mol in 1 dm^3. This requires an entropy of compression as high as $-26.58\,\mathrm{J \cdot K^{-1} \cdot mol^{-1}}$. Therefore, at 25°C,

$$\Delta G = \Delta G^\circ - RT\ln 24.46 = \Delta G^\circ - 7.93\,\mathrm{kJ} \tag{8}$$

The following considerations refer to the standard state (I), *i.e.* unit density number. This corresponds to Monte Carlo and molecular dynamics calculations performed in the isothermal-isobaric (*T*,*P*,*N*) ensemble, *i.e.* with fixed temperature, pressure, and number of molecules [63, 64].

Cavity formation

Since the venerable view of *van der Waals*, an intermolecular potential composed of repulsive and attractive parts is a fundamental ingredient of modern theories of the liquid state. Whereas the attractive interaction potential is not well known, the repulsive part, because of sharp changes with distance, is treatable by a common formalism in terms of the packing density η, which is the fraction of space occupied by the liquid molecules. The packing fraction is a key parameter in liquid state theories and is related in a simple way to the hard sphere (HS) diameter σ in a spherical representation of the molecules comprising the fluid, $\eta = \pi\rho\sigma^3/6 = \rho \cdot V_{\mathrm{HS}}$, where ρ is the number density $N/V =$ number of particles per unit volume and V_{HS} is the hard-sphere volume. Thus, by means of the molar liquid volume the packing fraction can be transformed into the HS diameter *via* $\eta = \pi\sigma^3 N_{\mathrm{A}}/(6V_{\mathrm{l}})$. When σ is in Å and V_{l} in cm^3, we have

$$\eta = \frac{0.3153\sigma^3}{V_l} \tag{9}$$

The energy of dissolution of an inert gas in a molecular liquid is the result of the compensation of a positive cavity formation energy, which is the reversible work required to open up a cavity in the fluid by pushing against the repulsive solvent hard cores, and the negative stabilization energy due to attractions:

$$\Delta G_{\mathrm{sol}} = \Delta G_{\mathrm{cav}} + \Delta G_{\mathrm{att}} \tag{10}$$

Since the cavity formation is a substantial part of the overall change in energy, much effort has been made towards an accurate calculation. HS theories only use two input parameters: d, which is the solute-solvent diameter ratio ($\sigma/\sigma_{\mathrm{s}}$), and the solvent packing fraction η. The first equation was proposed from the scaled particle theory (SPT) [65, 66]:

$$\frac{\Delta G_{\mathrm{cav}}}{RT} = \frac{2\eta^2 d^3}{(1-\eta)^3} + \frac{\eta d^2(2\eta d + 9/2)}{(1-\eta)^2} + \frac{\eta d(3 - 3d/2)}{1-\eta} + \eta d^3 - \ln(1-\eta) \tag{11}$$

The terminus SPT theory of fluids has been coined because it makes use of a coupling parameter which measures the size of a molecule and its potential field rather than the amplitude of this potential. A molecule is coupled formally to a fluid by letting it grow in size until it achieves the scale of its neighbours [65]. It is important to note that Eq. (10) is at variance with one frequently used, *e.g.* by *Graziano* [67, 68]. Thus, whereas *Graziano* calculated ΔG_{cav} for the solution of Ar in water to be 18.5 kJ/mol, Eq. (10) results in 30.9 kJ/mol, the latter being in agreement with the predictions of the equations given below.

The *Boublik-Mansoori-Carnahan-Starling-Leeland* (*BMCSL*) mixed hard-sphere equation of state has recently been shown to be somewhat superior to the SPT model in predicting the chemical potential of solvation in a HS fluid. The *BMCSL* cavity formation energy has the form [69, 70]

$$\frac{\Delta G_{\mathrm{cav}}}{RT} = 2\frac{\eta d^3}{(1-\eta)^3} + 3\frac{\eta d^2}{(1-\eta)^2} + 3\frac{\eta d(-d^2 + d + 1)}{(1-\eta)} + (-2d^3 + 3d^2 - 1)\ln(1-\eta) \tag{12}$$

Recently, this equation has been further improved by *Matyushov* and *Ladanyi* [71], rendering it also accurate for high densities of the liquid and large sizes of the solute:

$$\frac{\Delta G_{\text{cav}}}{RT} = \frac{3\eta}{(1-\eta)}d + \frac{3\eta(2-\eta)(1+\eta)}{2(1-\eta)^2}d^2 + \frac{\eta(1+\eta+\eta^2-\eta^3)}{(1-\eta)^3}d^3 - \ln(1-\eta) \tag{13}$$

In the application of these equations, the liquid HS diameter is a crucial parameter. For its determination, the most direct method is arguably that based on inert gas solubility data [72, 73]. However, in view of the arduousness involved and the uncertainties in both the extrapolation procedure and the experimental solubilities, it is natural to look out for alternatives. From the various suggestions [74, 75] a convenient way is to adjust σ such that the computed value of some selected thermodynamic quantity related to σ is consistent with experiment. This is, in fact, the best method up to now [76]. To diminish effects of attraction, the property chosen should probe primarily repulsive forces rather than attractions. Since the low compressibility of the condensed phase is due to short-range repulsive forces, the isothermal compressibility $\beta_T = -(1/V)(\partial V/\partial P)_T$ might be a suitable candidate in the framework of the generalized *vdW* equation of state, further implicating dipole–dipole forces [77]

$$\beta_T \frac{RT}{V_l}(\eta Z_0'(\eta) - Z_0(\eta) - 2Z_\mu(\eta) + 2Z) = 1 \tag{14}$$

where Z, Z_0, and Z_μ, respectively, are the compressibility factors of the real liquid, of the HS liquid according to *Charnahan* and *Starling*, and of dipole–dipole interactions in the framework of the mean spherical approximation (MSA). The HS diameters so determined are found to be in excellent agreement with those derived from inert gas solubilities [76]. It may be noted that the method of *Ben-Amotz* and *Willis* [78], also based on β_T, uses the nonpolar HS liquid as the reference and, therefore, is applicable only to liquids of weak dipole–dipole forces. Of course, as the reference potential approaches that of the real liquid, the HS diameter of the reference liquid approximates more closely the actual hard-core length. Finally, because of its popularity, an older method should be mentioned that relies on the isobaric expansibility α_p as the probe, but this method is inadequate for polar liquids. It turns out that solvent expansibility is appreciably determined by attractive forces.

In Table 3, some representative values of η and σ based on Eqs. (14) and (9), including the two extreme cases, are given. Actually, water and *n*-hexadecane have the lowest and highest packing density, respectively, of all common solvents. Summed up, for the time being, the cavity formation energy may be calculated from Eq. (13) with values of σ taken from Refs. [76] and [74], *i.e.* for water, $\eta = 0.412$ and $\sigma = 2.87$ Å. These values are higher than those often used ($\eta = 0.363$ and $\sigma = 2.75$ Å) [68]. For Monte Carlo simulations, the effective HS diameter for water will critically depend on the water model used [79].

It should be noted that under isochoric conditions the free energy of cavity formation is a totally entropic quantity, that is

$$T\Delta S_{\text{cav},V} = -\Delta G_{\text{cav}}, \quad \Delta S_{\text{cav},V} = -(\partial \Delta G_{\text{cav}}/\partial T)_V$$

Table 3. Packing densities in some liquids; data are taken from Ref. [14]

Liquid	η	Free volume (%)	σ (Å)
H_2O	0.41	59	2.87
n-C_6H_{14}	0.50	50	5.94
Benzene	0.51	49	5.27
MeOH	0.41	59	3.77
Et_2O	0.47	53	5.38
n-$C_{16}H_{34}$	0.62	38	8.33

For the isobaric case which is the usual experimental situation, the chemical potential divides into entropy and enthalpy,

$$\Delta G = \Delta H - T\Delta S_p, \quad \Delta S_p = -(\partial \Delta G/\partial T)_p$$

and

$$\Delta S_{\mathrm{cav},P} = \Delta S_{\mathrm{cav},V} + \rho\alpha_p(\partial \Delta G_{\mathrm{cav}}/\partial\rho)_T \tag{15}$$

The (positive) liquid expansibility term, however, is small for water due to its low expansibility ($\alpha_p = 0.26 \times 10^{-3}\,\mathrm{K}^{-1}$), as compared to ordinary liquids ($\alpha_p \cong 1.1-1.3 \times 10^{-3}\,\mathrm{K}^{-1}$). Along these lines, the large and negative entropy of cavity formation in water is traced to two particular properties of water: the small molecular size or, more specifically, the smaller size of the space between water molecules, and the low expansibility. The latter reflects the fact that chemical bonds cannot be stretched by temperature. There is also a recent perturbation approach showing that it is more costly to accommodate a cavity of molecular size in water than *e.g.* in hexane [80]. Considering the high fractional free volume for water (Table 3) it is concluded that the holes in water are distributed in smaller packets [81]. Compared to a H-bonding network, a hard-sphere liquid finds more ways to configure its free volume in order to make a cavity.

It may be mentioned that for the isobaric condition also cavity formation remains a quantity that is dominated by entropy. For example, ΔG_{cav} for methane in water is calculated to be 38.9 kJ/mol, which is made up of $\Delta H = 7.9$ kJ and $298\Delta S = 31.0$ kJ [82]. Thus the highly unfavourable cavity formation can be identified as a major contributor to the hydrophobic effect [83]. This can also be gauged from the solvation free energies of nitromethane as the solute in some aprotic solvents as shown in Table 4, where solvent ordering is, arbitrarily, according to the dielectric constant ε_s. The total solvation energy is a competition of the positive cavity formation energy and the negative solvation energy due to solute-solvent attractions (Eq. (10)). In the present case, only two kinds of attractions are relevant, that of dispersion and dipolar forces (neglecting quadrupolar forces, see below),

$$\Delta G_{\mathrm{att}} = \Delta G_{\mathrm{disp}} + \Delta G_{\mathrm{dipolar}} \tag{16}$$

For the methods of calculation, the reader may consult the original paper [82]. Table 4 shows that the contributions of cavity formation and dispersion, both appreciable, substantially cancel each other. The trend found between the overall solvation free energies and the dielectric properties of solute and solvent is an

Table 4. Thermodynamic potentials (kJ/mol) of dissolution of nitromethane at 25°C; data are taken from Ref. [82]

Solvent	ε_s	ΔG_{cav}	ΔG_{disp}	$\Delta G_{dipolar}$	ΔG(calc)	ΔG(exp)
n-C_6H_{14}	1.9	23.0	−32.9	−2.2	−12.1	−12.1
cyclo-C_6H_{12}	2.0	28.1	−38.1	−2.8	−12.7	−12.0
Et_3N	2.4	24.2	−33.5	−2.9	−12.2	−15.2
Et_2O	4.2	22.6	−33.4	−5.8	−16.5	−17.5
EtOAc	6.0	28.0	−38.5	−9.7	−20.1	−21.2
THF	7.5	32.5	−41.5	−12.2	−21.1	−21.3
Cyclohexanone	15.5	35.1	−39.8	−17.9	−22.6	−21.8
2-Butanone	17.9	28.3	−33.9	−18.9	−24.5	−21.9
Acetone	20.7	27.8	−31.2	−22.1	−25.5	−22.5
DMF	36.7	38.1	−32.1	−28.5	−22.5	−23.7
DMSO	46.7	41.9	−31.1	−31.0	−20.2	−23.6

outcome of this competition. It is now easy to imagine the changes to be expected if we switch over to a nonpolar solute to be dissolved in water. From the above, the cavity formation energies are dramatically increased. For instance, ΔG_{cav} for the nitromethane solute in water is calculated to be as high as 59.0 kJ/mol. On the other hand, dipolar forces can be neglected, of course, whereas the contribution of dispersion (see below) may well remain virtually unchanged [82]. This renders nonpolar substances very poorly soluble in water.

Solute–water and water–water correlations

A major difficulty in studying the effect of nonpolar solutes on water has, of course, been their low solubility. In this case any experimental signal – IR or otherwise – from the perturbed hydrating waters is masked by the much larger contribution from bulk water. Due to this fact, computer simulations have got ahead of experiment in studying the solute-induced perturbations in water structure. The result has been a wide range of competing models. In recent years, fortunately, the situation has changed dramatically due to the considerable improvements made to various experimental techniques. In this way molecular models derived from computer simulations are put on trial. It is gratifying that very diverse and independent experimental results suggest a fairly consistent picture of the local molecular order present in aqueous solutions.

(1) There is a well defined nearest neighbour hydration shell.
(2) Water molecules in the first coordination shell of nonpolar molecules tend to be tangentially orientated with respect to the surface of the former.
(3) The OH bonds perpendicular to the first coordination shell have the preference of forming linear H-bonds to outer-sphere water.
(4) The H-bonds of the water molecules in the immediate hydration zone appear to be somewhat stronger than in the bulk.
(5) Structural properties of water beyond the second solvation shell are similar to those of bulk water, *i.e.* longer range correlations are only weakly apparent.

Experimental evidence comes from neutron diffraction and isotopic substitution studies on solute/water samples pressurized to increase the concentration. The solutes used were argon [84], krypton [85], and methane [86]. The secondary structures are relatively weak, suggesting that the solute-water interaction is limited to the first hydration zone. The tangential orientation of the first-sphere waters follows from the coincidence of the first-peak positions of the solute-oxygen and solute-hydrogen PDFs. Such an edge-on arrangement of water molecules has also been reported to occur around the tetramethylammonium ion [87] and the methyl groups of tertiary butanol [88]. Another experiment involves FT-IR spectroscopy of water in the presence of trimethylamine-N-oxide, which is, by its positive hydration heat capacity, judged to be hydrophobic-like [89]. In agreement with the recent view of the water structure described above, the authors interpret the IR spectra in terms of two H-bond angle populations, a more distorted and a less distorted (more linear, *i.e.* ice-like) one, with the presence of hydrophobic groups increasing the population of the less distorted H-bonds. This corresponds to the classical structure enhancement, as indicated by a significant ^{1}H NMR low-field shift of the protons of water surrounding the alkyl group of ethanol [90] (but contradicted by a recent simulation study [91]). However, since it is restricted largely to the first hydration zone, the term 'microscopic iceberg' is less appropriate as it suggests three-dimensional structures. Better terms might be 'frozen patch' [92] or 'elasticated net' [93] (see below). The sphere in the vicinity of the cavity can synonymously be characterized in terms of the coordination number, since less distorted H-bonds mean that the coordination number of water, or the local density, is lowered compared to bulk water [58]. In view of the ambiguity of the coordination number in the case that non-nearest neighbours become important, it may more precisely be argued that the portion of *vdW*-bonded water molecules is reduced. This, in combination with strong attractive solute–water interactions, is ultimately the reason for the slowing down of the translational and rotational mobilities of water near a nonpolar solute. Experimental evidence is now available from NMR techniques [94–96], corroborating simulation results [97, 98]. Reverting to the edge-on arrangement of first-neighbour water molecules it is worth mentioning that the same conclusion has been reached by a variety of computer simulations, despite the divergent potential functions as well as different simulation times and methods of calculation employed [99–107].

Another peculiar feature of hydrophobicity is the at first unexpected strength of the water-solute interaction. The aforementioned term 'elasticated net' was coined by *Feakins et al.* [93] in their illuminating papers on the thermodynamics of solutions in order to picture the water structure around nonpolar groups. These authors argued that the large positive activation parameters found for the viscous flow in aqueous solutions require strong interactions to occur between the alkyl group and the solvent. More direct evidence of the peculiar action of water in caging hydrophobic solutes is apparent in the sensitive solvent dependence of the NMR chemical shift of ^{129}Xe, which is an effective probe of the hydrophobic environment [108]. It is remarkable that the shift in water is similar to that in benzene or olive oil, and hence is much greater than would be expected from the water's refractive index (note the linear trend between the gas-to-solution shift of ^{129}Xe and the refractive index function of common solvents [108]). Moreover, the shift is

much the same as the average of those found in the solid water clathrate. The relevance of this work is that it suggests not only that the xenon atom is caged in the water solution, but also that it is interacting in a noticeable fashion with the cage.

The occurrence of strong solute–water attractions follows, albeit indirectly, from Eq. (10), given that the favourable enthalpy in hydrophobic hydration is predominantly due to solute-water and not to water–water interactions and that the repulsive contributions can reliably be assessed from the HF formulas (Eqs. (11)–(13)). On the basis of the relationship $\Delta G_{\mathrm{att}} = \Delta G_{\mathrm{sol}} - \Delta G_{\mathrm{cav}}$, *de Souza* and *Ben-Amotz* [109] put forward that experimental solvation free energies typically represent a near cancellation of large repulsive and attractive contributions. Thus, higher values of ΔG_{cav} in water (due to the small water hard-core diameter) would correspond to more favourable attractions. As an example, whereas the results in water and *n*-hexane are qualitatively similar, the magnitudes of both parts are larger by a factor of about 2 in water. It may also be noted that values of ΔG_{att} so obtained have been found to correlate with the solute polarizabilities, suggesting a dispersive mechanism for attractive solvation, and are in fair agreement with dispersion energy estimates. Along these lines, the at first unusual experimental finding of increasing solubility of the noble gases with increasing size (in contrast to aliphatic hydrocarbons whose solubility decreases with size) can be rationalized [82]. This differential behaviour is straightforwardly explained in terms of the high polarizability of the heavy noble gases, having a large number of weakly bound electrons strengthening the *vdW* interactions with water. It can be shown that for noble gases of increasing size the *vdW* interactions increase more rapidly than the work of cavity creation, thus enhancing solubility; the opposite holds for hydrocarbons, thus lowering the solubility with increasing size [67].

In view of the ever increasing awareness of the importance of the dispersion component of non-ionic solvation, an adequate assessment is urgently required. For this purpose, the *LJ* potential as given by the first right-hand term in Eq. (1), albeit a simplification, is employed. The *LJ* potential may be viewed as an effective potential representing a rotationally averaged soft repulsive core and dispersive attractions of the molecules at contact. A salient case in revealing the significance of the nonpolar solute-water interaction is the numerical value of the *LJ* energy of water either extracted from experimental data or else needed in simulation work to reproduce the thermodynamic, structural, and dynamic characteristics of water. In a recent paper [74], *LJ* energies ε_{LJ} of molecular fluids have been recalculated using some updated methods. Experimental sources of ε_{LJ} are typically gas solubilities (GS), second virial coefficients (SVC), fluid viscosity, or liquid expansibilities. Of these, *LJ* energies extracted from GS data would seem to be the most reliable. The traditional procedure is based on *Pierotti's* theory giving $\varepsilon_{LJ}(\mathrm{H_2O}) = 79\,\mathrm{K}$ and $\sigma = 2.77\,\mathrm{\AA}$ (where, as in the following, ε_{LJ} is given as $\varepsilon_{LJ}/k_{\mathrm{B}}$) [110]. In this model, however, the effect of dispersions is treated in a continuum-like fashion. Another weak point is the manner of treating the repulsive contribution. A recalculation including cavity formation energy according to Eq. (12) and the *Barker-Henderson* theory for dispersion forces gives a much higher value of $\varepsilon_{LJ} = 332\,\mathrm{K}$ ($\sigma = 2.87\,\mathrm{\AA}$) [74].

Another method is based on the generalized *van der Waals* (G*vdW*) equation of state (Eq. (17)) where the liquid compressibility factor Z is composed of the

compressibility factor Z_0 for intermolecular repulsions, modeled by the HS potential, and the attraction forces term. Since, however, the *vdW* constant *a* involves the gross effect of the liquid attractions, contributions from other sources must at first be separated out. At present, this is adequately feasible only for dipole–dipole forces. Values of ε_{LJ} so obtained range from 57 to 846 K [74]. Furthermore, calculations from viscosity data afforded $\varepsilon_{LJ} = 808$ K ($\sigma = 2.64$ Å) [111]. Other values, ranging from 167 to 775 K, have been discussed by *Pierotti* [112]. Unfortunately, all *LJ* energies found in the literature suffer more or less from the problem of containing contributions from more than dispersion forces alone.

$$Z = PV/RT = Z_0(\eta) - \beta a \eta \tag{17}$$

Taken together, *LJ* energies extracted from GS data appear to be at present the least ambiguous choice for the following reasons: Firstly, a non-polar solute probes mainly the dispersion component of intermolecular attractions with dipolar and specific effects largely absent. Secondly, the free energies of dispersive forces, needed for the determination of liquid *LJ* energies from GS data, can adequately be calculated from *BH* and *WCA* theories. A disadvantage of the GS approach, however, is the necessity to employ arbitrary combining rules. It should be mentioned that upon using $\varepsilon_{LJ} = 332$ K in a thermodynamic analysis of hydration, and modifying the combining rules for larger solutes, the free energies of hydration for nonprotic solutes are well reproduced [82]. Beyond that, detailed comparisons with the *LJ* energy of water needed in simulation work to reproduce experimental data do not appear to be particularly valuable, since the numerical value to be chosen varies with the potential function employed [113]. Thus, for the TIP4P interaction potential of Eq. (1) the *LJ* parameters chosen were $\varepsilon_{LJ} = 88$ K and $\sigma = 3.15$ Å [114], and similarly for the TIP5P model, $\varepsilon_{LJ} = 80.6$ K and $\sigma = 3.12$ Å [41]. It should be remembered that the treatment of MD simulations is typically based on terms of the configuration of a pair of water molecules and does not (yet) take into consideration the aforementioned next-nearest neighbour aspect of liquid water. This raises serious questions about the realism of the results.

In conclusion, the relatively high ε_{LJ} value of liquid water as derived from the GS data (332 K) may be taken as another criterion for an enhanced nonpolar solute–water interaction. The physical basis for such strong interaction is intriguing. It has been suggested that the tangential ordering of O–H bonds of water molecules with respect to the surface of a non-polar solute might lead to enhanced proton tunneling (proton hopping), thereby creating a rapidly changing electric field that might strengthen the *London* dispersion interactions between water and the more polarizable solutes [67]. Thus, the interaction of the nonpolar group with its cage will not only be the sum of the *vdW* interactions of the group with the solvent molecules constituting the cage, but also be affected by the integrity of the cage.

In this context, it may be relevant to note that of the many crystalline clathrate hydrates known to date, guest molecules are always found to be separated by a single layer of shared solvent [115] as, for instance, in the helium hydrates [116]; a hydrophobic contact configuration of guest molecules has never been crystallized. This can well be indicative of the geometric constraints encountered by water molecules in an attempt to maintain a fully hydrogen bonded network surrounding the juxtaposed solutes. This is effected if the water molecules in the shell comprise

four bonds to other water molecules, three bonds forming the surface of a cage and one pointing outward. Small non-polar solutes may tend to occupy the same position with respect to the *quasi*-tetrahedral lattice, so that the more weakly interacting water (cf. Fig. 1) would, in effect, be competing for this mismatch site. The types of cages to be envisaged in aqueous solution may involve forms like those observed in the dimethylether hydrate [117]. For large nonpolar solutes, however, the intimate hydration mechanism may change as recently suggested [118] and disputed [119].

For computational studies, it has been shown recently that the performance of polarizable water force fields in calculating phase equilibria is improved dramatically by introducing an additional coupling of the intramolecular structure to the electronic environment [120]. To analyze the involvement of cooperative effects, the through-space coupling (TSC) concept, which is the molecular orbital representation of *vdW* repulsive-attractive forces [121], may be mentioned. Non-bonded (*vdW*) repulsion is a manifestation of covalent antibonding and can be reduced upon charge redistribution, *i.e.* if electron density is released from high-lying antibonding TSC orbitals. This approach should open opportunities for the further study of water structure and hydrophobic (as well as ionic) hydration.

Nonpolar vs. polar (ionic) hydration

As noted in the Introduction, the study of the hydration heat capacity ΔC_p should provide a deeper insight into the role of changes in water structure upon hydration than analysis of entropy or enthalpy changes alone. There are at least two reasons for this. Firstly, whereas the hydration of both nonpolar and ionic solutes is accompanied by a decrease in entropy, values of ΔC_p have the opposite sign, a large positive ΔC_p for hydration of non-polar groups and a negative one in the case of ionic solutes. Thus, explanations for the positive ΔC_p of hydrophobic hydration in terms of the induction of more ordered water which 'melts' at increasing temperatures do not explain the negative ΔC_p for polar and ionic species. The latter phenomenon is perhaps the more puzzling one in view of the negative entropies of ionic hydration. Secondly, heat capacity relates the other three major thermodynamic quantities describing solvation (ΔG, ΔH, ΔS; Eq. (18)) where $\langle \Delta E^2 \rangle$ is the mean-squared fluctuation in total energy and k is *Boltzmann's* constant. These four equivalent definitions of C_p illustrate the diverse thermodynamic implications for processes involving changes in C_p.

$$\Delta C_p = \frac{\partial \Delta H}{\partial T} = T \frac{\partial \Delta S}{\partial T} = -T^2 \frac{\partial^2 \Delta G}{\partial T^2} = \frac{\langle \Delta E^2 \rangle}{kT^2} \tag{18}$$

All recent explanations of the heat capacity puzzle are based on a two-state model of water structure. Before summarizing some relevant points, it is useful to compare the structural features of hydration of argon and the isoelectronic potassium cation, which differ dramatically with respect to the coordination number and the orientation of the hydrating water molecules. The argon atoms possess a nearest neighbour hydration shell composed of 16(2) water molecules in the range 2.8–5.4 Å, with the hydration shell molecules orientated with the dipole moment nearly tangentially to the Ar surface [84]. K^+, on the other hand, has 6–8

nearest neighbours at an internuclear K-O distance of 2.71–2.86 Å, with the hydrated water molecules, due to strong electrostatic solute-water interaction, directing their dipoles toward the central ion (with the M^+-O-H angle close to 127°) [122, 123].

Using a combination of Monte Carlo simulations and the random network model of water, *Sharp* and *Madan* [10, 124] have interpreted the IR spectra in terms of two major H-bond angle populations, a more distorted (more bent) and a less distorted (more linear, *i.e.* ice-like) one. The presence of hydrophobic groups increases the population of the less distorted H-bonds relative to the other, whereas polar and ionic solutes have the opposite effect. In addition, distortions in H-bond length and angle take place in a highly concerted fashion. Thus, the hydrogen bonds between the water molecules in the first hydration shell of a non-polar solute are shorter on average and less bent, giving rise to an increase in the water heat capacity whose sign is reversed for polar hydration. In terms of the last expression in Eq. (18), the water–water interaction contribution to ΔC_p is determined by the fluctuation in enthalpy given by the disparity in energy of different water microstates and the population of the energy levels. In other words, ΔC_p reflects the number of water molecules, *i.e.* the number of hydrogen bonds in the first shell, that are perturbed by the solute and further the extent of that perturbation. The positive sign of ΔC_p for non-polar hydration can be traced to (*i*) the fact that relatively many water molecules are engaged in the hydration shell and (*ii*) that the perturbation of the water structure is only weak so that the water molecules can fluctuate between these states. In the case of ion hydration, few water molecules are involved which, due to the strong electrostatic solute-water interaction, are so strongly associated with the solute that the water molecules cannot fluctuate easily between these states. Consequently, there is a net decrease in heat capacity.

The physical basis for the hydrophobic effect has also been studied using the statistical mechanical *MB* model of water in which the water molecules are represented as *Lennard-Jones* disks with hydrogen bonding arms [125] (the name of the *MB* model originates from the resemblance of each model water to the *Mercedes-Benz* logo). Similarly, the authors suggest a subdivision of the H-bonds in two classes which they call ‘circumferential waters’ and ‘radial waters’. The former are ‘cage waters’ forming H-bonds to neighbouring first-shell water molecules but not to the solute. It is found that the insertion of a non-polar solute into cold water causes ordering and strengthening of the H-bonds in the first shell, but the reverse applies in hot water. Based on simple geometrical considerations of hydrophobic hydration, *Matubayasi* differentiates between matching and mismatching water regions [126], the former being characterized by stronger H-bonds than the latter. Insertion of a hydrophobic solute induces a local environment which is favourable for the strengthening of H-bonds between the neighbouring water molecules. In other words, H-bonding networks are stabilized by the presence of guest molecules.

It should also be mentioned in this context that pressure increases the solubility [127]. The effect of pressure on the entropy has been examined, and it was found that increasing pressure causes a reduction of orientational correlations, in agreement with the idea of pressure as a ‘structure breaker’ in water. Actually, frozen clathrate hydrates trapped beneath oceans and arctic permafrost may contain

more than 50% of the world's organic carbon reserves [128, 129]. Likewise, the solubility of aromatics is increased at high pressure and temperature, with π-bond interactions involved [130].

Entropy-enthalpy compensation

Correlations between ΔH and ΔS known as the compensation effect are ubiquitous in physical chemistry [131–135], although the molecular origin remains obscure. In a simplified view, the origin of the compensation effect lies in the competing nature of maximum energy and minimum strain. Not unexpectedly, this phenomenon is also encountered in the thermodynamics of aqueous solutions. Thus, a linear trend between enthalpies and entropies of solution of quite diverse nonpolar gaseous solutes in water is apparent from Fig. 2. A closer view reveals that homologous series, or series of structurally similar compounds, separate into parallel straight lines (note the slightly deviating slope of the noble gases because they are monatomic and therefore lack degrees of freedom). This is particularly evident in Fig. 3, where also polar and protic solutes are included.

A very instructive example of enthalpy–entropy compensation is found in the thermodynamics of transfer of argon from cyclohexane as a reference solvent to water and to hydrazine (Table 5) [136]. Whereas the enthalpies and entropies are obviously very different, they almost completely compensate each other, rendering

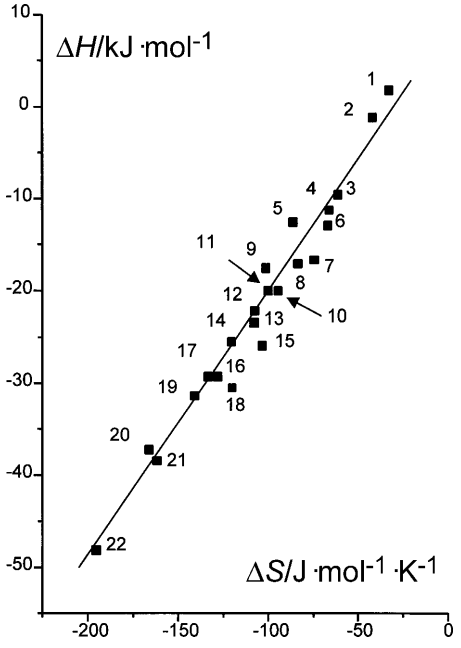

Fig. 2. Thermodynamics of solution of gaseous solutes in water at 298 K. The solutes are He (1), Ne (2), Ar (3), Kr (4), Xe (5), CF_4 (6), SF_6 (7), CH_4 (8), C_2H_6 (9), C_3H_8 (10), *i*-C_4H_{10} (11), *n*-C_4H_{10} (12), Me_4C (13), *n*-C_5H_{12} (14), *c*-C_5H_{10} (15), *n*-C_6H_{14} (16), Me_4Sn (17), *c*-C_6H_{12} (18), *n*-C_7H_{16} (19), *n*-C_8H_{18} (20), Et_4C (21), and Et_4Sn (22). Data are taken from *Abraham MH*, *Nasehzadeh A* (1981) J. Chem. Soc., Faraday Trans. 1 **77**: 321. Note that a correction for the enthalpy of sublimation or evaporation has been applied to non-gaseous solutes

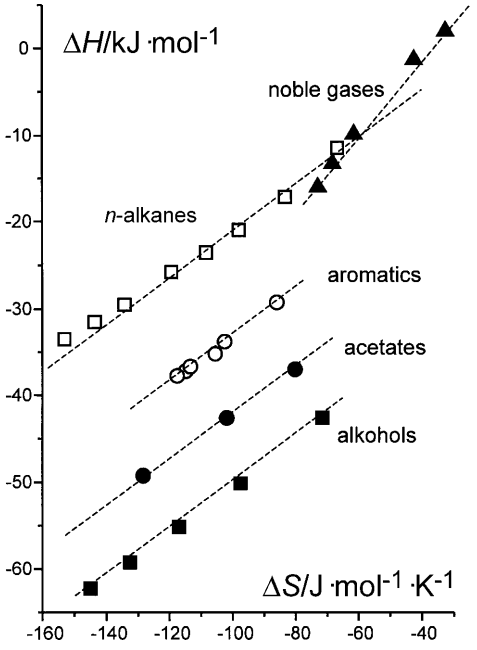

Fig. 3. Thermodynamics of solution of gaseous solutes in water at 298 K; data are taken from Ref. [82]; note that a correction for the enthalpy of sublimation/evaporation has been applied where necessary

Table 5. Thermodynamic data for the transfer of argon from cyclohexane to water and to hydrazine at 25°C; data are taken from Ref. [136]

Transfer of 1 mol Ar	$\frac{\Delta G_{tr}}{kJ/mol}$	$\frac{\Delta H_{tr}}{kJ/mol}$	$\frac{298\Delta S_{tr}}{kJ/mol}$
$C_6H_{12} \rightarrow N_2H_4$	11.88	9.50	−2.37
$C_6H_{12} \rightarrow H_2O$	10.38	−11.21	−21.58

the *Gibbs* free energies of transfer very similar. Since both solvents are hydrogen bonded, the peculiar nature of water cannot simply result from hydrogen bonding. Rather, water is unique by its molecular structure, having the same number of donors (protons) and acceptors (lone pairs) arranged tetrahedrally. This allows water to form a cage around a nonpolar solute without sacrificing much of the H-bonding. Moreover, the water structure can close on the solute like an elastic net, trapping the solvent and bringing the molecules close to it, enhancing their mutual *vdW* interactions. These could well be comparable in strength with the water–water interactions they replace [93]. Of course, the exothermic solute–solvent interaction occurs at the expense of orientational strain of the water cage. In contrast to water, hydrazine, due to its structure, is not a good cage former, rendering the transfer of argon from cyclohexane endothermic but, to compensate, entropically not so unfavourable. At higher temperatures water also gradually loses its tendency to form cages. On the other hand, cavity formation becomes less severe. Note that in

going from 25 to 100°C the HS diameter σ of water changes from 2.87 to 2.51 Å, and the packing fraction η from 0.412 to 0.267 [137, 78]. Thus, on the basis of Eq. (13), ΔG_{rep} reduces from 38.9 to 23.5 kJ/mol, *i.e.* the solution of inert gases becomes less favourable by enthalpy but more favourable by entropy in a compensatory manner. This is reflected by the solubility data of methane in water as displayed in Table 2. It can be seen that the free energy is much less sensitive to temperature than are either enthalpy and entropy.

Another factor supporting enthalpy-entropy compensation is implicit in the curious agreement between the calculated and experimental ebullioscopic and cryoscopic constants. As is known from first-course physical chemistry, the theoretical derivation of these constants relies on the assumption that the free energy of the solvent varies with the number but not the nature of dissolved solute molecules [138].

Unfortunately, a detailed analysis of experimental enthalpy-entropy data such as those presented in Figs. 2 and 3 has not yet been set about; the problem may be approached in a way similar to that taken by *Linert* and *Jameson* in the treatment of isoparametric relationships [139]. What is eagerly being sought instead is to separate the hydrophobic process into individual steps by model calculations, looking for compensation behaviour of sub-systems, especially that of solvent reorganization, which may be defined as the difference of the average solvent–solvent interaction energy with and without the presence of the solute. On the basis of thermodynamic and statistical mechanical arguments it has been argued that the solvent reorganization energy and entropy exhibit complete cancellation [140, 48, 49].

Grundwald's arguments [48] proceed as follows: When solute B is dissolved in solvent A,

$$\mathrm{B}(g) \leftrightarrow \mathrm{B}(a) \tag{19}$$

the solvent is affected such that ($s_{\mathrm{B}} =$ mean coordination number of B)

$$\mathrm{B}(g) + s_{\mathrm{B}}\mathrm{A}(a) \leftrightarrow \mathrm{B}(a) + s_{\mathrm{B}}\mathrm{A}(b) \tag{20}$$

where A(a) denotes molecules A surrounded by A, and A(b) denotes molecules A in the neighbourhood of B. This equation is divisible into two parts:

$$\begin{aligned} &\mathrm{B}(g) \leftrightarrow \mathrm{B}(a) && \text{nominal equation} \\ &s_{\mathrm{B}}\mathrm{A}(a) \leftrightarrow s_{\mathrm{B}}\mathrm{A}(b) && \text{environmental equation} \end{aligned}$$

In terms of mole numbers,

$$n_{\mathrm{B}(a)} = n_{\mathrm{B}} \quad \text{B in the environment of A} \tag{21a}$$

$$n_{\mathrm{A}(b)} = s_{\mathrm{B}} n_{\mathrm{B}} \quad \text{A in the environment of B} \tag{21b}$$

$$n_{\mathrm{A}(a)} = n_{\mathrm{A}} - s_{\mathrm{B}} n_{\mathrm{B}} \quad \text{A in the environment of A} \tag{21c}$$

Thus,

$$G = n_{\mathrm{A}(a)} G_{\mathrm{A}(a)} + n_{\mathrm{A}(b)} G_{\mathrm{A}(b)} + n_{\mathrm{B}(a)} G_{\mathrm{B}(a)} \tag{22a}$$

or

$$G = (n_{\mathrm{A}} - s_{\mathrm{B}} n_{\mathrm{B}}) G_{\mathrm{A}(a)} + s_{\mathrm{B}} n_{\mathrm{B}} G_{\mathrm{A}(b)} + n_{\mathrm{B}} G_{\mathrm{B}(a)} \tag{22b}$$

and

$$G = n_{\mathrm{A}} G_{\mathrm{A}(a)} + s_{\mathrm{B}} n_{\mathrm{B}} (G_{\mathrm{A}(b)} - G_{\mathrm{A}(a)}) + n_{\mathrm{B}} G_{\mathrm{B}(a)} \tag{22c}$$

Allowing s_{B} to relax to equilibrium (*le Châtelier's* principle) with n_{A}, n_{B}, T, p constant,

$$\left(\frac{\partial G}{\partial s_{\mathrm{B}}} \right)_{n_{\mathrm{A}}, n_{\mathrm{B}}} = n_{\mathrm{B}} (G_{\mathrm{A}(b)} - G_{\mathrm{A}(a)}) = 0$$

gives

$$\Delta G_{\mathrm{env}} \equiv G_{\mathrm{A}(x)} - G_{\mathrm{A}(a)} = 0 \tag{23}$$

Hence,

$$\Delta H_{\mathrm{env}} = T \Delta S_{\mathrm{env}} \tag{24}$$

According to other treatments, however, the solvent reorganization energy and entropy certainly partly compensate but do not cancel each other [141, 142]. It is important to note, however, that discussion about cancellation between portions of the excess entropy and energy of solution is, to some extent, semantic, as pointed out by *Lee* [143]. Some of the reasons for the different results are a matter of physical interpretation, mathematical manipulation, and conditions chosen [144]. For instance, the analysis by *Yu* and *Karplus* [49] refers to solute insertion at constant volume (and not pressure). As another minor point, the thermal motion of the solute has not been considered (which is, however, unimportant in the case of water) [142b]. Anyway, the basic problem seems to rest on the artificial apportionment of both energy and entropy. Albeit the evaluation of solvent reorganization, with enthalpy-entropy compensation involved, is of fundamental interest by itself, it should be kept in mind that it ultimately features just a subsystem of the hydrophobic effect whose overall enthalpy and entropy arguably do vary in some compensatory manner.

As a first approximation, the net compensation behaviour can be described on the basis of the fundamental decoupling of the (total, *i.e.* experimental) solvation enthalpy into direct and response components [82]

$$\Delta H = \Delta H_{\mathrm{sw}} + \Delta H_{\mathrm{ww}} \tag{25a}$$

where the first term represents the solute–water interaction energy as the direct enthalpic perturbation and the second term is the enthalpy change due to the solvent reorganization that happens as a result of the perturbation. The situation with entropy is trickier. Basically, all entropy change upon hydration is due to solvent reorganization. If, however, one considers the excluded volume effect of cavity formation as independent of water structure, a dissection analogously to the above may be envisaged:

$$\Delta S = \Delta S_{\mathrm{sw}} + \Delta S_{\mathrm{ww}} \tag{25b}$$

Whereas the reorganization components are still unavailable theoretically for real systems, there are schemes for calculating both ΔH_{sw} and ΔS_{sw}. Most notable is the linear relationship found between ΔH_{sw}, calculated by direct temperature differentiation of the dispersive chemical potential, and ΔS_{sw}, assessed by means of Eq. (15), for nonpolar solutes. This result is at the origin of the hydrophobic effect

and reflects the opposite effect exerted by solute size on cavity formation and on the attractive solute–water interaction. Whilst an increase in solute size enhances the cavity formation energy, polarizability is also increased, and this leads to a stronger solute–water attraction. Ultimately, compensation behaviour follows from the fact that cavity formation largely determines the excess entropy, whereas dispersive forces determine the excess enthalpy. These features appear to be the basis for the success of surface area correlations for hydrophobic phenomena [145, 146].

Another interesting result concerns the values of ΔH_{ww} and ΔS_{ww} as obtained by subtraction of the solute-solvent parts from experimental enthalpies and entropies, $\Delta H_{ww} = \Delta H^{exp} - \Delta H_{sw}$ and $\Delta S_{ww} = \Delta S^{exp} - \Delta S_{sw}$, in that there is an exact equality between ΔH_{ww} and $298\Delta S_{ww}$ in accordance with Eq. (24). This is all the more meaningful as both parts are derived from equations (and theories) that are fully independent of one another.

However, there is also a less pleasant feature in this analysis in that the calculated values of both ΔH_{ww} and ΔS_{ww} are positive and unexpectedly high (*e.g.* $\Delta H_{sw} = -21.55$ kJ/mol and $\Delta S_{sw} = -98.1$ J/K · mol for the methane/water system); this would point to H-bond weakening. Along with the experimental data of Table 1 one obtains $\Delta H_{ww} = +10$ kJ/mol and $\Delta S_{ww} = +31.4$ J/K · mol. On the other hand, the orientational rearrangement of vicinal water molecules in forming the water cage should be negative in entropy. Furthermore, according to the experimental and theoretical evidence described above, the water structure beyond the second solvation layer may be considered as rather unperturbed relative to the first hydration zone. This latter finding, by the way, might explain the relative success of continuum water models [52, 147–151]. It has therefore to be concluded that the calculation scheme of cavity formation for water should be modified so as to include the rearrangement of the vicinal water molecules [152]. Suggestions to modify SPT are not new [153]. Basically, it seems questionable whether positional and orientational entropies can really be decoupled.

The "Like-Dissolves-Like" Rule

In some respects, the phenomenon behind the like-dissolves-like rule is the converse of the hydrophobic effect. The buzzword 'polarity', derived from the dielectric approach to solvent effects, is certainly the most popular word dealing with solvent effects. However, the famous rule of thumb *similia similibus solvuntur* (like-dissolves-like), applied when discussing solubility and miscibility, has many exceptions. For instance, methanol and toluene, with ε_s of 32.6 and 2.4, respectively, are miscible, as are water (78.4) and isopropanol (18.3). The problem lies in exactly what is meant by a 'like' solvent. Originally, the term 'polarity' was meant to be an abbreviation of 'static dipolarity' and was thus associated with the dielectric properties of the solvent only.

Clearly, neither the dielectric constant nor the dipole moment is an adequate means to define polarity. The reason is that there are liquids whose constituent molecules have no net dipole moment, for symmetry reasons, but nevertheless have local polar bonds. This is quite obvious by a comparison of *E*-1,2-dichloroethene (formerly *trans*-1,2-dichloroethylene) with *Z*-1,2-dichloroethene (formerly *cis*-1,2-

dichloroethylene). The former has a molecular dipole moment of $\mu = 1.76\,\mathrm{D}$ and $\varepsilon_s = 9.20$, whereas the latter has $\mu = 0\,\mathrm{D}$ and $\varepsilon_s = 2.14$, but the polarity of the carbon-chlorine bonds are certainly the same in both cases. A polar molecule can be defined as having a strongly polar bond, but need not necessarily be a dipole. Recently, there has been growing awareness of the significant contributions of higher multipoles to intermolecular forces, of which the quadrupole moment is of primary importance. For the polarity of the C–H bonds it should be remembered that electronegativity is not an intrinsic property of an atom, but instead varies with hybridization. Only the $C(sp^3)$-H bond can be considered as truly nonpolar, but not the $C(sp^2)$–H bond [154]. Finally, ethine has hydrogen atoms which are definitely acidic.

It should be mentioned that higher moments or local polarities cannot produce a macroscopic polarization and thus be detected in infinite wavelength dielectric experiments yielding a static dielectric constant close to the squared refractive index. Because of their short range, quadrupolar interactions do not directly contribute to the dielectric constant, but are only reflected in the *Kirkwood* g_K factor which decreases due to breaking the angular dipole-dipole correlations with increasing quadrupolar strength.

As is well known, the dipole moment of an uncharged body can be thought of as being formed by separating positive and negative charges, the magnitude of the dipole being the product of charge and separation. Similarly, the quadrupole moment of a system with zero dipole moment can be thought of as arising from a separation of equal and opposite dipoles, the magnitude of a quadrupole being proportional to the product of dipole moment and separation. Thus, the linear carbon dioxide molecule possesses a quadrupole moment, the two C–O dipoles being opposed to but separated from one another. Similarly, any linear molecules, even dihydrogen or dioxygen, and planar ones, such as boron trifluoride and benzene, are quadrupolar. On the other hand, regular tetrahedral molecules like methane and carbon tetrachloride have octupoles as their leading multipoles, and octahedral ones like sulfur hexafluoride possess hexadecapoles [155].

Beyond this it should be remarked that many liquids have both a dipole and a quadrupole moment (water for example). In a recent perturbation theory study of solvation thermodynamics it has been shown that small solute dipoles are even more effectively solvated by solvent quadrupoles than by solvent dipoles [156]. Whereas for dipolar solvents such as acetonitrile, acetone, and dimethyl sulfoxide the dipolar solvation mechanism will be prevailing, for less dipolar solvents like tetrahydrofurane quadrupoles and dipoles might equally contribute to the solvation energetics. According to the *Matyushov-Voth* theory [156], the ratio of the quadrupolar solvation energy E_q to the dipolar solvation energy E_d is approximately equal to

$$\frac{E_q}{E_d} \approx 2.0 \frac{Q^2}{m^2 \sigma^2} r_{0s}^{-4/3} \tag{26}$$

where Q is the solvent quadrupole moment, m is the solvent dipole moment, $r_{0s} = r_0/\sigma + 0.5$ is the reduced distance of closest approach of the solute and solvent hard cores, r_0 is the solute radius, and σ is the HS diameter of the solvent. It has also been calculated that the effect of quadrupolar forces on various thermo-

dynamic properties is much greater than dipolar forces at comparable parameter values [157, 158]. For the ion-hydration problem, it has been proposed recently to use a hybrid potential in which the ion-water interaction is modeled by ion-dipole plus ion-quadrupole terms [159]. In doing so, a bifurcated H-bond structure around the anion (two hydrogens are equally bonded), which is a consequence of the monopole-dipole potential, was avoided. Finally, the aforementioned problem with calculating the dispersion solvation component in the framework of *LJ* parameters, *i.e.* the necessity to employ arbitrary combining rules, should be recalled. It has long ago been suggested, but in the meantime forgotten, that the failure of the common combination rules $\varepsilon_{1,2} = (\varepsilon_1 \cdot \varepsilon_2)^{1/2}$ and $\sigma_{1,2} = (\sigma_1 + \sigma_2)/2$ for *LJ* parameters corresponding to the interaction of dissimilar pairs of molecules [160] is at least partly due to the neglection of quadrupolar effects [155].

The interplay (from classical theories unexpectedly strong) between the π-electron cloud of an aromatic system (or any other π system such as alkenes) with a cation is called cation-π interaction. This is an electrostatic binding largely determined by ion-quadrupole interactions. For instance, the gas-phase binding energy between K^+ and benzene of -77 kJ/mol is even slightly higher than that of K^+ and water at -75 kJ/mol [161]. In addition, this interaction is size-dependent: whereas in the case of K^+_{aq} benzene will displace some water molecules from direct contact with the ion, Na^+_{aq} is resistant towards dehydration in an aromatic environment, giving rise to selectivity in some K^+-channel proteins. Recently, this type of interaction has been hypothesized to play important roles in molecular recognition [162]. Similarly, the interactions of benzene with Li^+, BeH^+, and LiH were calculated by *ab initio* SCF and MO theory to be quite exothermic, *i.e.* -353, -193, and -572 kJ/mol, respectively [163]. Even between atomic lithium and benzene a significant electronic interaction takes place [164]. Consideration of quadrupole–quadrupole interactions also improves the description of solid–solid and solid–fluid equilibria in a molecular model of benzene [165]. Furthermore, the mutual solubilities of water and aromatic hydrocarbons, as measured by IR spectroscopy, are increased in high temperature/pressure mixtures [166], and this may be explained in these terms.

In the light of these findings it is strongly recommended to redefine polarity [14]. Instead of meaning solely dipolarity, it should also include higher multipolar properties, *i.e.* polarity = dipolarity + quadrupolarity + octopolarity.

Solvents which comprise molecules with permanent dipole moment of small or zero magnitude but with finite higher-order multipoles are called nondipolar in the literature [167, 168]. As to the relative importance of each contribution, it should be noted that the interaction energy decreases more rapidly the higher the order of the multipole. Thus, for the interaction of an *n*-pole with an *m*-pole, the potential energy varies with distance according to $E \propto 1/(r^{n+m+1})$. The reason for the faster decrease is that the array of charges seems to blend into neutrality more rapidly with distance the higher the number of individual charges contributing to the multipole. Therefore, quadrupolar forces die off faster than dipolar forces on the one hand, and on the other hand, are more important than the higher multipole forces.

The implication of quadrupolarity finally reconciles the notorious troublemakers in solvent reactivity correlations, the aromatic and chlorinated solvents (in

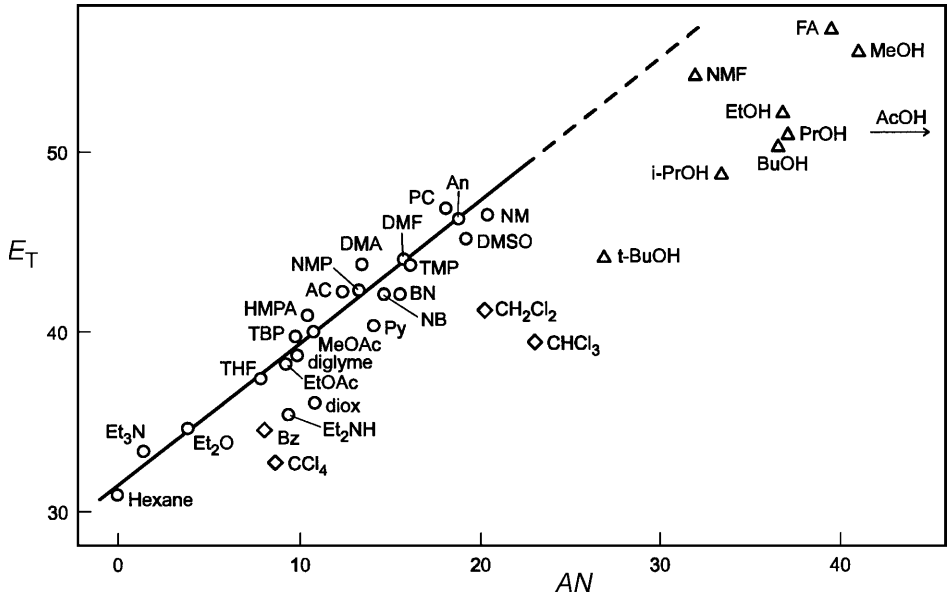

Fig. 4. Relationship between the $E_T(30)$ values and the acceptor number; triangles: protic solvents, squares: aromatic and chlorinated solvents; data are taken from Ref. [14]

addition to the protic solvents). A typical plot is shown in Fig. 4 relating two famous empirical solvent parameters ($E_T(30)$ and acceptor numbers). Originally, the deviations of the aromatic and chlorinated solvents have been interpreted in terms of polarizability effects. This gave rise to the addition of a polarizability correction term in the LSFERs (linear solvation free energy relationships) [14]. However, in a thermodynamic analysis of some empirical polarity scales in terms of long-range solute–solvent interactions due to induction, dispersion, and dipole–dipole forces, the deviations remained, although polarizability effects were properly taken into account [169]. Thus, two alternative explanations for the exceptional behaviour of the aromatic and chlorinated solvents are conceivable: charge transfer (solute–solvent π orbital overlap resulting in exciplex formation) or solute–quadrupole interactions. Although the authors of Ref. [71] were biased in favour of the former, the latter possibility appears to be preferable [168]. The quadrupole and charge transfer mechanisms, reflecting inertial and inertialess solvation pathways, could be distinguished by a comparative analysis of absorption and fluorescence shifts. In terms of quadrupolarity, the discrepant solvent classes of the aromatic and chlorinated solvents in Fig. 4 are due to a size effect. Thus, the betaine-30 molecule, which is the probe dye for the $E_T(30)$ scale, is much larger in size than triethyl phosphine oxide, which forms the basis of the acceptor number scale. Therefore, quadrupolar solvent-dipolar solute interactions are more important at the latter polarity scale. In other words, quadrupolar (and octupolar) solvents have a higher solvating power according to the *AN* relative to the $E_T(30)$ value.

Also, the so-called dioxane anomaly [170] (this solvent appears as a polar solvent despite of a very low dielectric constant) can be rationalized partly in terms of the high quadrupole moment of dioxane. In addition, it appears that dioxane can communicate its polar nature over a relatively long spatial extent, either because of

the large charge separation in dioxane itself or because of strong intermolecular interactions between dioxane molecules [171].

Another phenomenon arguably related to quadrupolarity is the high solubility of O_2 in perfluorocarbons (*PFC*), of which the most investigated ones are perfluorodecaline, perfluorotripropylamine, and perfluorooctyl bromide. Intravenously administered *PFCs* may become an essential part in allogeneic transfusion sparing strategies, including preoperative autologous predonation, acute normovolemic hemodilution, and intraoperative blood recovery [172]. Though still awaiting confirmation, the most probable solution mechanism is the interaction between the negative charges on the fluorine centers and the dioxygen quadrupole moment, leading to an additional attractive stabilization. Thus, a variety of examples have been presented leading to the assumption that quadrupolar solvent effects on solvation and reactivity will receive increasing attention in the future [173, 174].

Notwithstanding the modified definition of polarity (*vide supra*), the problem remains that positive and negative charge solvation are not distinguished. Most importantly, there is no general relationship between polarity and cation solvation tendency. For example, although nitromethane and *DMF* have the same dielectric constant, the extent of ion pairing in $MeNO_2$ is much greater than that in *DMF*. This observation is attributed to the weak basicity of $MeNO_2$ which poorly solvates cations. As a result, ion pairing is stronger in $MeNO_2$ in spite of the fact that long-range ion-ion interactions in the two solvents are equal.

Finally, a potential problem with polarity rests in the fact that this term is typically associated with enthalpy. But caution is urged in interpreting the like-dissolves-like rule in terms of enthalpy. It has often been stated for example that non-polar liquids such as octane and carbon tetrachloride are miscible because the molecules are held together by weak dispersion forces. However, the importance of entropy may not be forgotten in the spontaneous mixing of the two phases.

References

[1] Ben-Naim A (1980) Hydrophobic Interactions. Plenum, New York
[2] Evans DF, Ninham BW (1986) J Phys Chem **90**: 226
[3] Tanford C (1973) The Hydrophobic Effect: Formation of Micelles and Biological Membranes. Wiley, New York
[4] Dill KA (1990) Biochemistry **29**: 7133
[5] Førrisdahl OK, Kvamme B, Haymet ADJ (1996) Mol Phys **89**: 819
[6] Wang H, Ben-Naim A (1996) J Med Chem **39**: 1531
[7] Ashbaugh HS, Kaler EW, Paulaitis ME (1999) J Am Chem Soc **121**: 9243
[8] Battino R, Clever HL (1966) Chem Rev **66**: 395
[9] Ben-Naim A, Marcus Y (1984) J Chem Phys **81**: 2016
[10] Madan B, Sharp K (1996) J Phys Chem **100**: 7713
[11] Lazaridis T (1998) J Phys Chem B **102**: 3531
[12] Marmur A (2000) J Am Chem Soc **122**: 2120
[13] Blokzijl W, Engberts JBFN (1993) Angew Chem Int Ed Engl **32**: 1545
[14] Schmid R (2001) Solvent Effects on Chemical Reactivity. In: Wypych G (ed) Handbook of Solvents. ChemTec Publishing, Toronto, p 737
[15] Giguère PA (1984) J Raman Spectrosc **15**: 354
[16] Wall TT, Hornig DF (1965) J Phys Chem **43**: 2079
[17] Walrafen GE (1968) J Chem Phys **48**: 244

[18] D'Arrigo G, Maisano G, Mallamace F, Migliardo P, Wanderlingh F (1981) J Chem Phys **75**: 4264
[19] Giguère PA (1987) J Chem Phys **87**: 4835
[20] Walrafen GE, Fisher MR, Hokmabady MS, Yang W-H (1986) J Chem Phys **85**: 6970
[21] a) Hare DE, Sorensen CM (1990) J Chem Phys **93**: 25; b) Hare DE, Sorensen CM (1990) J Chem Phys **93**: 6954; c) Hare DE, Sorensen CM (1992) J Chem Phys **96**: 13
[22] Maréchal Y (1991) J Chem Phys **95**: 5565
[23] Libnau FO, Toft J, Christy AA, Kvalheim OM (1994) J Am Chem Soc **116**: 8311
[24] Soper AK, Phillips MG (1986) Chem Phys **107**: 47
[25] Svishchev IM, Kusalik PG (1993) J Chem Phys **99**: 3049
[26] Svishchev IM, Zassetsky AY (2000) J Chem Phys **112**: 1367
[27] Soper AK (1994) J Chem Phys **101**: 6888
[28] De Santis A, Rocca D (1997) J Chem Phys **107**: 9559
[29] Giguère PA (1984) J Raman Spectrosc **15**: 354
[30] Némethy G, Scheraga HA (1962) J Chem Phys **36**: 3382
[31] Bosio L, Chen S-H, Teixeira J (1983) Phys Rev A **27**: 1468
[32] Sciortino F, Geiger A, Stanley HE (1990) Phys Rev Lett **65**: 3452
[33] Robinson GW, Cho CH, Urquidi J (1999) J Chem Phys **111**: 698
[34] Vedamuthu M, Singh S, Robinson GW (1994) J Phys Chem **98**: 2222 and references therein
[35] Kamb B (1964) Acta Cryst **17**: 1437
[36] Kamb B, Hamilton WC, LaPlaca SJ, Prakash A (1971) J Chem Phys **55**: 1934
[37] Benson SW, Siebert ED (1992) J Am Chem Soc **114**: 4269
[38] Falk M, Ford TA (1966) Can J Chem **44**: 1699
[39] Giguère PA, Pigeon-Gosselin M (1986) J Raman Spectrosc **17**: 341
[40] Cho CH, Singh S, Robinson GW (1997) J Chem Phys **107**: 7979
[41] Mahoney MW, Jorgensen WL (2000) J Chem Phys **112**: 8910
[42] Arthur JW, Haymet ADJ (1998) J Chem Phys **109**: 7991
[43] Frank HS, Evans MW (1945) J Chem Phys **13**: 507
[44] Mizuno K, Miyashita Y, Shindo Y, Ogawa H (1995) J Phys Chem **99**: 3225
[45] Goldammer EV, Hertz HG (1970) J Phys Chem **74**: 3734
[46] Pottel R, Kaatze V (1969) Ber Bunsenges Phys Chem **73**: 437
[47] Silveston R, Kronberg B (1989) J Phys Chem **93**: 6241
[48] Grunwald E, Steel C (1995) J Am Chem Soc **117**: 5687
[49] Yu HA, Karplus M (1988) J Chem Phys **89**: 2366
[50] Qian H, Hopfield JJ (1996) J Chem Phys **105**: 9292
[51] Lee B (1985) J Chem Phys **83**: 2421
[52] Vaisman II, Brown FK, Tropsha A (1994) J Phys Chem **98**: 5559
[53] Re M, Laria D, Fernández-Prini R (1996) Chem Phys Lett **250**: 25
[54] Soper AK, Finney JL (1993) Phys Rev Lett **71**: 4346
[55] Turner J, Soper AK (1994) J Chem Phys **101**: 6116
[56] Soper AK, Luzar A (1996) J Phys Chem **100**: 1357
[57] Meng EC, Kollman PA (1996) J Phys Chem **100**: 11460
[58] Ikeguchi M, Seishi S, Nakamura S, Shimizu K (1998) J Phys Chem B **102**: 5891
[59] Ben-Naim A (1987) Solvation Thermodynamics. Plenum, New York
[60] Abraham MH (1982) J Am Chem Soc **104**: 2085
[61] Ben-Naim A (1978) J Phys Chem **82**: 792
[62] Schmid R, Miah AM, Sapunov VN (2000) Phys Chem Chem Phys **2**: 97
[63] Owicki JC, Scheraga HA (1977) J Am Chem Soc **99**: 7403
[64] Bridgeman CH, Buckingham AD, Skipper NT (1996) Chem Phys Lett **253**: 209
[65] Reiss H (1966) Adv Chem Phys **9**: 1
[66] de Souza LES, Stamatopoulou A, Ben-Amotz D (1994) J Chem Phys **100**: 1456

[67] Graziano G (1998) J Chem Soc Faraday Trans **94**: 3345
[68] Graziano G (1999) Phys Chem Chem Phys **1**: 1877
[69] Boublik T (1970) J Chem Phys **53**: 471
[70] Mansoori GA, Carnahan NF, Starling KE, Leland Jr TW (1971) J Chem Phys **54**: 1523
[71] Matyushov DV, Ladanyi BM (1997) J Chem Phys **107**: 5815
[72] a) Pierotti RA (1963) J Phys Chem **67**: 1840; b) Pierotti RA (1976) **76**: 717
[73] a) Wilhelm E, Battino R (1971) J Chem Phys **55**: 4021; b) Wilhelm E, Battino RJ (1971) J Chem Thermodyn **3**: 761; Wilhelm E, Battino RJ (1973) J Chem Phys **58**: 3558
[74] Matyushov DV, Schmid R (1996) J Chem Phys **104**: 8627
[75] Ben-Amotz D, Herschbach DR (1990) J Phys Chem **94**: 1038
[76] Schmid R, Matyushov DV (1995) J Phys Chem **99**: 2393
[77] Matuyshov DV, Schmid R (1994) J Phys Chem **98**: 5152
[78] Ben-Amotz D, Willis KG (1993) J Phys Chem **97**: 7736
[79] Floris FM, Selmi M, Tani A, Tomasi J (1997) J Chem Phys **107**: 6353
[80] Prévost M, Oliveira IT, Kocher JP, Wodak SJ (1996) J Phys Chem **100**: 2738
[81] Pohorille A, Pratt LR (1990) J Am Chem Soc **112**: 5066
[82] Matyushov DV, Schmid R (1996) J Chem Phys **105**: 4729
[83] Stamatopoulou A, Ben-Amotz D (1998) J Chem Phys **108**: 7294
[84] Broadbent RD, Neilson GW (1994) J Chem Phys **100**: 7543
[85] Filipponi A, Bowron DT, Lobban C, Finney JL (1997) Phys Rev Lett **79**: 1293
[86] De Jong PHK, Wilson JE, Neilson GW, Buckingham AD (1997) Molec Phys **91**: 99
[87] Turner JZ, Soper AK, Finney JL (1995) J Chem Phys **102**: 5438
[88] Bowron DT, Finney JL, Soper AK (1998) J Phys Chem B **102**: 3551
[89] Sharp KA, Bhupinder M, Manas E, Vanderkooi JM (2001) J Chem Phys **114**: 1791
[90] Mizuno K, Miyashita Y, Shindo Y, Ogawa H (1995) J Phys Chem **99**: 3225
[91] Fidler J, Rodger PM (1999) J Phys Chem B **103**: 7695
[92] Guillot B, Guissani Y, Bratos S (1991) J Chem Phys **95**: 3634
[93] a) Feakins D, Canning FM, Mullally JJ, Waghorne WE (1989) Pure Appl Chem **61**: 133; b) Feakins D, Bates FM, Waghorne WE, Lawrence KG (1993) J Chem Soc Faraday Trans **89**: 3388
[94] Holz M, Haselmeier R, Mazitov RK, Weingärtner H (1994) J Am Chem Soc **116**: 801
[95] Haselmeier R, Holz M, Marbach W, Weingärtner H (1995) J Phys Chem **99**: 2243
[96] Nakahara M, Wakai C, Yoshimoto Y, Matabayasi N (1996) J Phys Chem **100**: 1345
[97] Sciortino F, Geiger A, Stanley HE (1992) J Chem Phys **96**: 3857
[98] García-Tarrés L, Guàrdia E (1998) J Phys Chem B **102**: 7448
[99] Owicki JC, Scheraga HA (1977) J Am Chem Soc **99**: 7413
[100] Swaminathan S, Harrison SW, Beveridge DL (1978) J Am Chem Soc **100**: 5705
[101] Geiger A, Rahman A, Stillinger FH (1979) J Chem Phys **70**: 263
[102] Pangali C, Rao M, Berne J (1979) J Chem Phys **71**: 2982
[103] Alagona G, Tani A (1980) J Chem Phys **72**: 580
[104] Rapaport DC, Schegara HA (1982) J Am Chem Soc **86**: 873
[105] Vaisman II, Brown FK, Tropsha A (1994) J Phys Chem **98**: 5559
[106] Hernández-Cobos J, Ortega-Blake I (1995) J Chem Phys **103**: 9261
[107] Fois E, Gamba A, Redaelli C (1999) J Chem Phys **110**: 1025
[108] a) Miller KW, Reo NV, Uiterkamp AJMS, Stengle DP, Stengle TR, Williamson KL (1981) Proc Natl Acad Sci USA **78**: 4946; b) Stengle TR, Hosseini SM, Basiri HG, Williamson KL (1984) J Solution Chem **13**: 779
[109] de Souza LES, Ben-Amotz D (1994) J Chem Phys **101**: 9858
[110] Pierotti RA (1976) Chem Rev **76**: 717
[111] Reid CR, Prauznitz JM, Poling BE (1987) The Properties of Gases and Liquids. McGraw-Hill, New York
[112] Pierotti RA (1965) J Phys Chem **69**: 281

[113] Jorgensen WL, Chandrasekhar J, Madura JD, Impey RW, Klein ML (1983) J Chem Phys **79**: 926
[114] Lazaridis T, Karplus M (1996) J Chem Phys **105**: 4294
[115] Zichi DA, Rossky PJ (1985) J Chem Phys **83**: 797
[116] a) Londono D, Kuhs WF, Finney JL (1988) Nature **332**: 141; b) Londono D, Finney JL, Kuhs WF (1992) J Chem Phys **97**: 547
[117] Udachin KA, Ratcliffe CI, Ripmeester JA (2001) Angew Chem **113**: 1343
[118] Southall NT, Dill KA (2000) J Phys Chem B **104**: 2391
[119] a) Graziano G (2001) J Phys Chem B **105**: 2079; b) Southall NT, Dill KA (2001) J Phys Chem B **105**: 2082
[120] Chen B, Xing J, Siepmann JI (2000) J Phys Chem B **104**: 2391
[121] Sapunov VN, Kirchner K, Schmid R (2001) Coord Chem Rev **214**: 143
[122] Marcus Y (1988) Chem Rev **88**: 1475
[123] Ohtaki H, Radnai T (1993) Chem Rev **93**: 1157
[124] a) Sharp K, Madan B (1997) J Phys Chem B **101**: 4343; b) Madan B, Sharp K (1997) J Phys Chem B **101**: 11237
[125] Silverstein KAT, Haymet ADJ, Dill KA (1999) J Chem Phys **111**: 8000
[126] Matubayasi N (1994) J Am Chem Soc **116**: 1450
[127] Rick SW (2000) J Phys Chem B **104**: 6884
[128] Collett TS (1997) Chem Eng News **75**: 60
[129] Silverstein TP (1998) J Chem Educ **75**: 116
[130] Furutaka S, Ikawa S (1998) J Chem Phys **108**: 5159
[131] a) Linert W (1989) Chem Phys **129**: 381; b) Linert W, Jameson RF (1989) Chem Soc Rev **18**: 477; c) Linert W (1994) Chem Soc Rev **23**: 429
[132] Boots HMJ, de Bokx PK (1989) J Phys Chem **93**: 8240
[133] Vailaya A, Horváth C (1996) J Phys Chem **100**: 2447
[134] Stolov AA, Herrebout WA, van der Veken BJ (1998) J Am Chem Soc **120**: 7310
[135] Abraham MH, Whiting GS, Fuchs R, Chambers EJ (1990) J Chem Soc Perkin Trans **2**: 291
[136] Ramadan MS, Evans DF, Lumry R (1983) J Phys Chem **87**: 4538
[137] Matyushov DV, Schmid R (1994) Ber Bunsenges Phys Chem **98**: 1590
[138] Atkins PW (1990) Physical Chemistry, 4th edn. Oxford University Press, Oxford, p 167ff
[139] Linert W, Jameson RF (1993) J Chem Soc Perkin Trans **2**, 1415
[140] Ben-Naim A (1978) J Phys Chem **82**: 874
[141] Matubayasi N, Reed LH, Levy RM (1994) J Phys Chem **98**: 10640
[142] a) Lazaridis T (1998) J Phys Chem B **102**: 3531; b) Lazaridis T (2000) J Phys Chem B **104**: 4964
[143] a) Lee B (1994) Biophys Chem **51**: 271; b) Lee B (1995) Methods in Enzymol **259**: 555
[144] a) Smith DE, Laird BB, Haymet ADJ (1993) J Phys Chem **97**: 5788; b) Lazaridis T, Paulaitis ME (1993) J Phys Chem **97**: 5789
[145] Ashbaugh HS, Kaler EW, Paulaitis ME (1999) J Am Chem Soc **121**: 9243
[146] Murray JS, Abu-Awwad F, Politzer P (1999) J Phys Chem A **103**: 1853
[147] Rashin AA, Bukatin MA (1991) J Phys Chem **95**: 2942
[148] Pitarch J, Moliner V, Pascual-Ahuir JL, Silla E, Tuñón I (1996) J Phys Chem **100**: 9955
[149] Sitkoff D, Ben-Tal N, Honig B (1966) J Phys Chem **100**: 2744
[150] Bader JS, Cortis CM, Berne BJ (1997) J Chem Phys **106**: 2372
[151] Luo R, Moult J, Gilson MK (1997) J Phys Chem B **101**: 11226
[152] Guillot B, Guissani Y (1993) J Chem Phys **99**: 8075
[153] Stillinger FH (1973) J Solution Chem **2**: 141
[154] Bratsch SG (1988) J Chem Edu **65**: 34
[155] Buckingham AD (1959) Quart Rev Chem Soc **13**: 183
[156] Matyushov DV, Voth GA (1999) J Chem Phys **111**: 3630
[157] Patey GN, Valleau JP (1976) J Chem Phys **64**: 170

[158] Jiang S, Pitzer KS (1995) J Chem Phys **102**: 7632
[159] Liu Y, Ichiye T (1996) J Phys Chem **100**: 2723
[160] Cottrell TL, Hamilton RA, Taubinger RP (1956) Trans Faraday Soc **52**: 1310
[161] a) Carbacos OM, Weinheimer CJ, Lisy JM (1998) J Chem Phys **108**: 5151; b) Carbacos OM, Weinheimer CJ, Lisy JM (1999) J Chem Phys **110**: 8429
[162] Siu FM, Ma NL, Tsang CW (2001) J Am Chem Soc **123**: 3397
[163] Jemmis ED, Schleyer PVR (1982) J Am Chem Soc **104**: 4781
[164] Manceron L, Andrews L (1988) J Am Chem Soc **110**: 3840
[165] Schroer JW, Monson PA (2001) J Chem Phys **114**: 4124
[166] Furutaka S, Ikawa S (1998) J Chem Phys **108**: 5159
[167] a) Perng BC, Newton MD, Raineri FO, Friedman HL (1996) J Chem Phys **104**: 7153; b) Perng BC, Newton MD, Raineri FO, Friedman HL (1996) J Chem Phys **104**: 7177
[168] Reynolds L, Gardecki JA, Frankland SJV, Horng ML, Maroncelli M (1996) J Phys Chem **100**: 10337
[169] Matyushov DV, Schmid R, Ladanyi BM (1997) J Phys Chem B **101**: 1035
[170] Geerlings JD, Varma CAGO, Hemmert MCv (2000) J Phys Chem B **104**: 56
[171] Kauffman JF (2001) J Phys Chem A **105**: 3433
[172] Zuck TF, Riess JG (1994) Crit Rev Clin Lab Sci **31**: 295
[173] Jeon J, Kim HJ (2000) J Phys Chem A **104**: 9812
[174] Read I, Napper A, Zimmt MB, Waldeck DH (2000) J Phys Chem A **104**: 9385

Received May 8, 2001. Accepted (revised) May 23, 2001